ELSEVIER

NeuroImage

www.elsevier.com/locate/ynimg
NeuroImage 25 (2005) 1292–1301

Functional representation of the finger and face in the human somatosensory cortex: intraoperative intrinsic optical imaging

Katsushige Sato,[a,*] Tadashi Nariai,[b] Yoji Tanaka,[b] Taketoshi Maehara,[b] Naohisa Miyakawa,[a] Shinichi Sasaki,[a] Yoko Momose-Sato,[a] and Kikuo Ohno[b]

[a]*Department of Physiology, Tokyo Medical and Dental University Graduate School and Faculty of Medicine, 1-5-45 Yushima, Bunkyo-ku, Tokyo 113-8519, Japan*
[b]*Department of Neurosurgery, Tokyo Medical and Dental University Graduate School and Faculty of Medicine, Bunkyo-ku, Tokyo 113-8519, Japan*

Received 2 November 2004; revised 13 December 2004; accepted 17 December 2004
Available online 17 February 2005

We applied the intrinsic optical imaging technique to the human primary somatosensory cortex during brain tumor/epilepsy surgery for nine patients. The cortical surface was illuminated with a Xenon light through an operating microscope, and the reflected light, which passed through a 605 nm bandpass filter, was detected by a CCD camera-based optical imaging system. Individual electrical stimulation of five digits induced changes in the reflected light intensities. Visualizing the intrinsic optical responses, we constructed maps of finger representation in Brodmann's area 1. In the maps, response areas of Digits I to V were sequentially aligned along the central sulcus in the crown of the postcentral gyrus from the latero-inferior region (Digit I) to the medio-superior region (Digit V). The neighboring response areas partially overlapped each other, as previously described in the monkey somatosensory cortex. Similar results were obtained in the face region with stimulation of the three branches of the trigeminal nerve. These results suggest that the overlap of the response areas is a common feature in the somatosensory cortex not only in monkeys, but also in humans.

Keywords: Finger; Face; Human somatosensory cortex

Introduction

Intrinsic optical imaging is a useful technique for monitoring brain function with high spatial and temporal resolutions (Bonhoeffer and Grinvald, 1996). Since the pioneering work by Grinvald et al. (1986), it has been applied to the cat/monkey visual cortex (Bonhoeffer and Grinvald, 1993; Chapman et al., 1996; Gödecke and Bonhoeffer, 1996; Ts'o et al., 1990), the rodent somatosensory cortex (Dowling et al., 1996; Gochin et al., 1992; Masino et al., 1993; Tanaka et al., 2000; Yazawa et al., 2001), and the rodent spinal cord (Sasaki et al., 2002, 2003). The intrinsic optical signals (changes in reflected light intensity) are considered to consist of three different components: they originate from (1) activity-dependent changes in the oxygen saturation level of hemoglobin, (2) changes in blood volume in an area containing electrically active neurons, and (3) light-scattering changes that accompany cortical activation, which are caused by ion/water movement, expansion and contraction of extracellular spaces, capillary expansion, or neurotransmitter release (Bonhoeffer and Grinvald, 1996; Cohen, 1973; Frostig et al., 1990; Malonek and Grinvald, 1996).

The intrinsic optical imaging technique was also applied to the human cortex during neurosurgical operations. Haglund et al. (1992) first demonstrated the usefulness of this technique for monitoring stimulation-evoked epileptiform afterdischarges and cognitively-evoked functional activity. Subsequently, it was used to monitor brain functions related to sensation (Cannestra et al., 1998; Sato et al., 2002; Shoham and Grinvald, 2001; Toga et al., 1995) and language tasks (Cannestra et al., 2000; Pouratian et al., 2000). In most studies of sensation, optical signals were evoked by median/ulnar nerve stimulation or digit stimulation. Although these studies showed that different peripheral stimulation provided different functional maps, contiguous representation of fine receptive fields, such as response areas of the five digits, was not assessed.

The purpose of this study was to examine functional representation of the finger area in the human primary somatosensory cortex. In the human somatosensory cortex, Penfield and Boldray (1937) first described a somatosensory homunculus on the postcentral gyrus. In the monkey, using a micro-electrode recording technique, Kaas et al. (1979) showed that complete somatotopic maps also present in each Brodmann's area (3a, 3b, 1, and 2). In the monkey somatosensory cortex, significant overlaps of functional representation of the fingers were described in somato-

* Corresponding author. Fax: +81 3 5803 0118.
E-mail address: katsushige.phy2@tmd.ac.jp (K. Sato).
Available online on ScienceDirect (www.sciencedirect.com).

1053-8119/$ - see front matter © 2004 Elsevier Inc. All rights reserved.
doi:10.1016/j.neuroimage.2004.12.049

topic maps, and we questioned whether similar overlaps exist in the human brain. In the present study, we also examined functional representation of the three branches of the trigeminal nerve, and compared the data between the finger and face regions.

Materials and methods

Subjects

We measured intrinsic optical signals from the somatosensory cortex in nine anesthetized patients undergoing surgery for frontal, parietal, or temporal lobe brain tumors (eight patients) and temporal lobe epilepsy (one patient). The patient data are summarized in Table 1. The patients had no past history of neurosurgical operations. All the patients were right-handed. Informed consent was obtained from all patients prior to the surgery and intraoperative intrinsic optical imaging. The patients were anesthetized with isoflurane, and the head was fixed to the operating table via a three point fixation Mayfield apparatus. Craniotomy and dura opening were performed, and the surface of the cerebral cortex around each lesion was exposed.

Before the intrinsic optical imaging, we recorded cortical somatosensory-evoked potentials (SEPs) in response to median nerve stimulation with a four-channel cortical electrode. It has been reported that a phase reversal of the negative peak of SEPs occurs across the central sulcus (Nuwer et al., 1992). Using the SEPs, we identified the central sulcus as a landmark.

Peripheral nerve stimulation

For the optical imaging, Digits I–V (for five patients), the supraorbital branch of the ophthalmic nerve (N. V_1), the zygomaticofacial branch of the maxillary nerve (N. V_2) and the mental branch of the mandibular nerve (N. V_3) (for two patients) were stimulated transcutaneously with surface electrodes driven by an electrical stimulator. In two patients (Case 1 and Case 5 in Table 1), only Digit I or Digits I and II were stimulated, and further stimulation was ceased because optical responses were not clear. The stimuli, consisting of ten pulses, were delivered at 5 Hz for 2 s with an interstimulus interval of 20 s. The stimulation intensity was 10 mA, which produced the maximal SEP responses in the somatosensory cortex. Bonhoeffer and Grinvald (1993) reported that stimulation longer than 2 s caused large blood vessel artifacts in the optical maps, presumably due to larger contributions of activity-dependent changes in blood volume and blood flow. In the present study, we could not test multiple stimulation paradigms for the optical imaging because of the limited recording time during neurosurgical operations and used a single stimulation paradigm as described above.

Intraoperative intrinsic optical imaging

After identifying the central sulcus, the recording site of the cerebral cortex was stabilized with a glass plate. This procedure minimized brain movements in the *Z* axis, as well as in the *X* and *Y* planes. No significant brain damage was observed due to this procedure after neurosurgical operations, although the possibility that the plate could affect the local brain environment, including blood flow, cannot be excluded. The somatosensory cortex was illuminated using a Xenon lamp driven by a stable DC power supply via an operating microscope (Carl Zeiss, Inc., Thornwood, NY). The depth of focus of the operating microscope was set to about 500 μm under the cortical surface. Reflected light from the cortex was passed through interference filters of different wavelengths. The filter used for visualizing the surface of the cortex and its vascular pattern had a transmission maximum at 540 ± 30 nm, and the filter used for intrinsic imaging had a passband at 605 ± 5 nm (Asahi Spectra Co., Tokyo, Japan). We used this wavelength (605 nm) for two reasons. First, it coincides with the peak of the difference spectra between oxy-hemoglobin and deoxy-hemoglobin, and maximizes the contribution of oximetry signals relative to other intrinsic signals (Bonhoeffer and Grinvald, 1993; Frostig et al., 1990). Second, in our previous studies on the rat somatosensory cortex (Tanaka et al., 2000; Yazawa et al., 2001), brainstem (Yazawa et al., 1999), and spinal cord (Sasaki et al., 2002), we detected the largest intrinsic signal at a wavelength of 605 nm. In the present study, we could not examine the wavelength dependency of the optical signals because of the limited recording time (about 30 min).

Intrinsic imaging was performed using a differential video acquisition system IMAGER 2001 (Optical Imaging, Germantown, NY) via a charge coupled device camera (CS8310B, Tokyo, Tokyo Denshi Instrument Co., Japan) fitted to an operating microscope. This camera has a spatial resolution of 648 × 480 pixels. Three (for face stimulation) or five (for finger stimulation) recording

Table 1
Summary of patient data

Case	Sex	Age (years)	Diagnosis	Lesion	Stimulation site	IOS
1	M	60	glioblastoma	rt. frontoparietal	lt. 1st digit	nd
2	F	19	low grade astrocytoma + intractable epilepsy	lt. temporal	rt. V_1–V_3 nerve	+
3	M	30	oligodendroglioma	lt. parietal	rt. V_1–V_3 nerve	+
4	F	38	oligodendroglioma	rt. frontal	lt. 1st–5th digit	+
5	M	62	metastatic brain tumor	lt. parietal	rt. 1st/2nd digit	+, map (−)
6	F	57	metastatic brain tumor	lt. parietal	rt. 1st–5th digit	+
7	F	69	metastatic brain tumor	rt. frontal	lt. 1st–5th digit	+
8	F	24	temporal lobe epilepsy	lt. temporal (epileptic focus)	rt. 1st–5th digit	+, map (−)
9	M	47	oligodendroglioma	lt. frontoparietal	rt. 1st–5th digit	+

IOS: intrinsic optical signal, nd: not detected, map (−): functional maps were not obtained (see text).

sessions were allowed for each patient. One recording session consisted of six blocks. Each block consisted of four stimulation trials and two non-stimulation (control) trials interlaced randomly, with an inter-trial interval of 20 s. During each trial, eleven optical images were collected over 5.0 s and stored on a computer with data acquisition software VDAQ (Optical Imaging, Germantown, NY). For stimulation trials, Digits I–V, or the supraorbital, zygomaticofacial and mental nerves, were stimulated for 2 s from the onset of data acquisition. Optical reflectance images were represented by a fractional change ($\Delta R/R$) to correct for uneven illumination using a data analyzing software program WinMix (Optical Imaging, Germantown, NY). To make functional maps of the finger and face representations in the somatosensory cortex, we defined an optical response area as an area with the fractional change ($\Delta R/R$) > 1.5×10^{-3}.

Results

Optical responses induced by Digits I–V stimulation

Fig. 1 shows intrinsic optical images obtained from a 47-year-old patient who suffered from an oligodendroglioma (Case 9 in Table 1). All of the right digits (Digits I–V) were stimulated individually by ring-like electrodes, and intrinsic optical signals (optical reflectance changes) were detected from the left somatosensory cortex. Prior to the intrinsic optical recording, we recorded cortical somatosensory-evoked potentials (SEPs) in response to right median nerve stimulation to identify the central sulcus (indicated by a yellow line in the right panel). The recording site is shown on a three-dimensionally reconstructed magnetic resonance (MR) image with a blue rectangle and on a photograph of the cortical surface with a red ellipse. The recording site corresponded to the postcentral gyrus (primary somatosensory cortex (SI)) (right panels of Fig. 1). The detected reflectance signals were illustrated by a pseudo-color image, in which a decrease in light reflectance was shown from green to red, and they were superimposed on a vascular image. In these images, the optical responses induced by Digits I–V stimulation were clearly identified in different regions of the primary somatosensory cortex.

Fig. 2 illustrates another example of intrinsic optical images obtained with Digits I–V stimulation in a 38-year-old patient who suffered from an oligodendroglioma (Case 4 in Table 1). Left Digits I–V were individually stimulated, and optical signals were detected from the right somatosensory cortex. Similar to Case 9 shown in Fig. 1, electrical stimulation of the individual digits evoked optical responses at different, but sequential, regions in the somatosensory cortex. In this case, as shown in the lower right panels in Fig. 2, the brain tumor was located in the premotor cortex and partially invaded into the motor cortex. After brain tumor resection, although the patient transiently experienced severe paresis of hands and legs for 2 weeks, no sensory disturbance of the fingers was observed.

In three other patients whose fingers were electrically stimulated (Cases 1, 5 and 8 in Table 1), we could not make functional maps of finger representation in the somatosensory cortex. Case 1 (glioblastoma) presented total paresis of the left extremities with loss of the SEP responses, and optical responses were not evoked by Digit I stimulation (data not shown). We therefore stopped the intraoperative optical imaging. In Case 5 (metastatic brain tumor), we detected optical signals with Digits I and II stimulations, as shown in Fig. 3A. However, in the region corresponding to the Digit III–V areas, the arachnoid membrane was thickened, and this produced spurious signals which did not vary with the site of stimulation (arrowheads in Fig. 3A). Fig. 3B shows the estimated optical response areas for Digits I and II in red and yellow, respectively. In Case 8 (temporal lobe epilepsy), we clearly detected optical responses with Digit I stimulation (data not shown). However, this response area was located near the edge of the operation area. Since the regions corresponding to the Digit II–V areas seemed to be located outside the operation area, we ceased the optical measurement.

Functional mapping of finger representation in the somatosensory cortex

Fig. 4 shows functional maps of finger representations in the somatosensory cortex obtained from four different subjects. In this figure, we defined the optical response area for each finger stimulation as the area with the fractional change ($\Delta R/R$) > 1.5×10^{-3}. The response areas of different fingers are shown with different translucent colors, and are superimposed on the vascular image. In the present study, we only analyzed results qualitatively, and did not quantitatively or statistically compare the detected areas between the subjects. The reasons were as follows; (1) in some subjects, the brains were more or less transformed due to the brain tumor; (2) the anesthetic state was not exactly the same between the subjects; and (3) part of the response area was located outside the detected field (e.g., the Digit V response area of Cases 6 and 7 in Fig. 4).

In Fig. 4, we extracted the following characteristics of the optical response patterns: (1) Digits I to V stimulation induced optical responses which were sequentially aligned along the central sulcus in the crown of the postcentral gyrus; (2) the Digit I area was located in the most latero-inferior region, and the Digit V area was located in the most medio-superior region; (3) in most cases, the Digit I area was the largest and the Digit III–V areas were smaller; (4) the neighboring response areas partially overlapped each other, as illustrated with mixed colors.

In Fig. 4, the extent of overlapping areas showed inter-individual variations. Especially in Case 4, the areal overlapping appeared larger than in other cases. As stated in the previous section, the brain tumor in Case 4 was located very close to the recording site, this might have caused the transformation of the somatosensory cortex and functional representation of the finger region.

Mapping of face representation in the somatosensory cortex

To examine whether similar characteristics of functional maps were observed in other regions of the primary somatosensory cortex, we applied the optical imaging technique to the face region in two patients. Fig. 5A illustrates intrinsic optical images obtained with supraorbital (N. V_1), zygomaticofacial (N. V_2), and mental (N. V_3) nerve stimulation in a patient who suffered from a low-grade astrocytoma (Case 2 in Table 1). The recording site is shown with a red circle on a photograph of the cortical surface, which corresponded to the postcentral gyrus (right panels of Fig. 5A). The detected reflectance signals were illustrated by a pseudo-color image and were superimposed on a vascular image (left panels of Fig. 5A). In these images, the optical responses induced by supraorbital, zygomaticofacial, and mental nerve stimulation were clearly detected from different areas along the central sulcus.

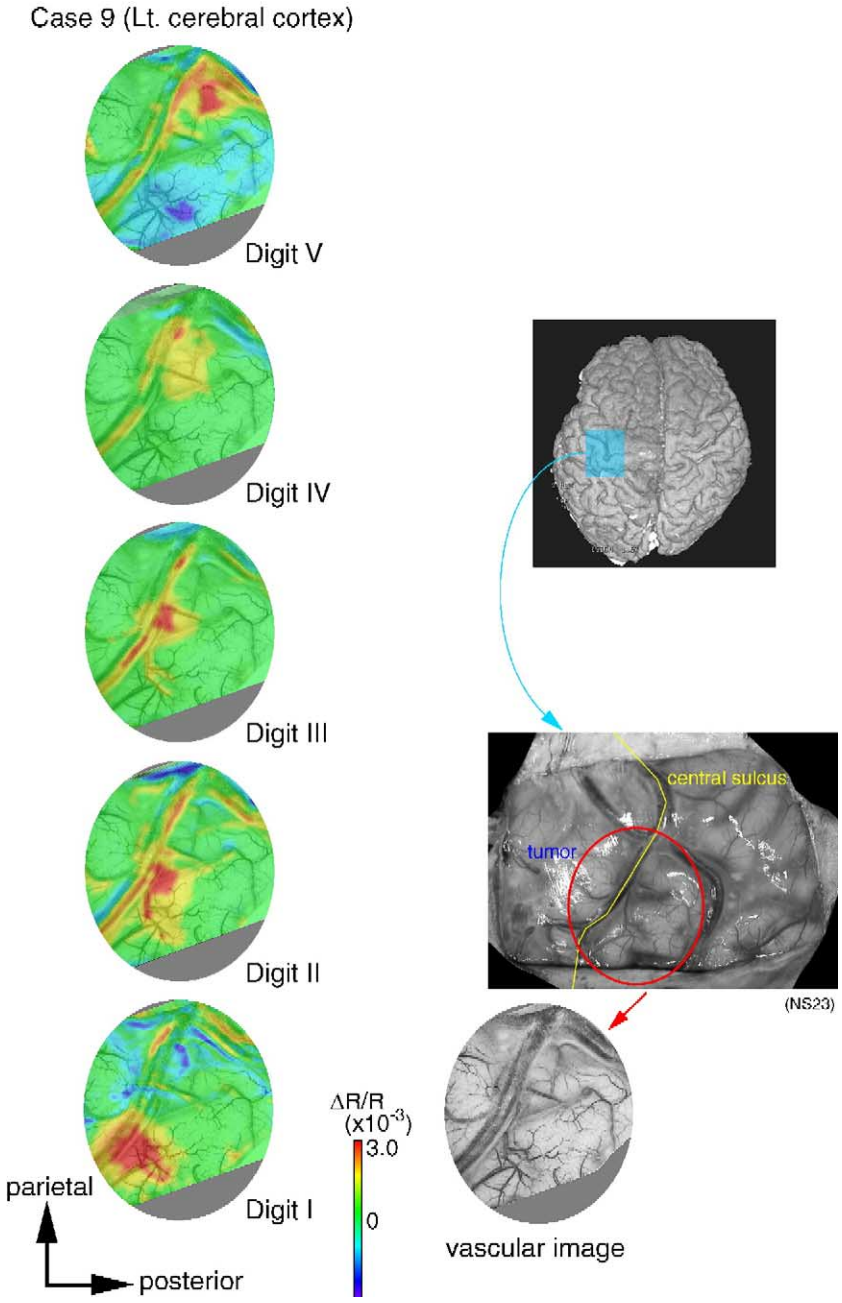

Fig. 1. Intrinsic optical responses induced by Digits I–V stimulation. Right Digits I to V were individually stimulated, and intrinsic optical signals were recorded from the left somatosensory cortex of a 47-year-old patient (Case 9 in Table 1). The detected optical responses are illustrated by pseudo-color images superimposed on the vascular image (left panels). The recording site is shown on a three-dimensionally reconstructed magnetic resonance (MR) image with a blue rectangle and on a photograph of the cortical surface with a red ellipse. The yellow line indicates the central sulcus. The central sulcus was determined by recording somatosensory evoked potentials (SEPs) in response to median nerve stimulation. The vascular image obtained at a wavelength of 540 nm is also shown in the lower right panel.

Next, we determined the optical response area for each nerve stimulation as the area with the fractional change $(\Delta R/R) > 1.5 \times 10^{-3}$. The response areas of different nerves are shown with different translucent colors in Fig. 5B. In this figure, we showed two examples of functional maps obtained from two patients (Case 2 and Case 3 in Table 1). As in the case with finger stimulation, optical response areas induced by supraorbital, zygomaticofacial, and mental nerve stimulation partially overlapped each other, although the extent of the overlap was smaller than that in the finger region (see Discussion).

Discussion

In the present study, we performed intraoperative intrinsic optical imaging for nine patients, and succeeded in recording

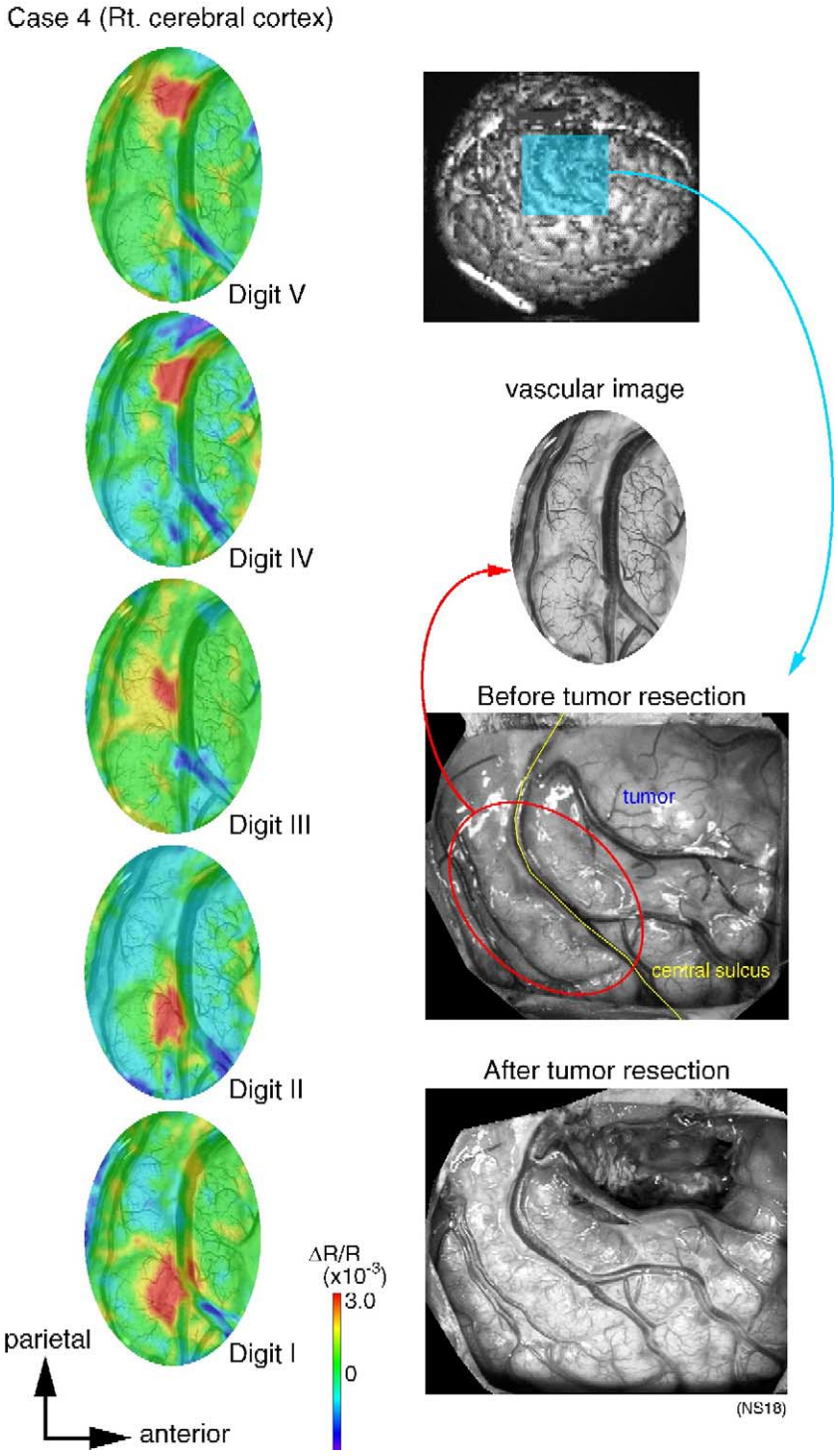

Fig. 2. Another example of intrinsic optical responses induced by Digits I–V stimulation. The left panels show intrinsic optical responses obtained from the right somatosensory cortex of a 38-year-old patient (Case 4 in Table 1). In the right panels, the recording site is shown on a three-dimensionally reconstructed MR image with a blue rectangle and on a photograph of the cortical surface with a red ellipse. In this case, a brain tumor (oligodendroglioma) was located in the premotor cortex. Photographs taken before and after resection of the tumor are shown on the lower right.

optical responses from eight patients as shown in Table 1. From six patients, we could obtain clear functional maps of the finger or face area in the somatosensory cortex. We discuss here the functional representation of the finger and face in the somatosensory cortex, and also consider a limitation in the application of intraoperative intrinsic optical imaging.

Functional representations of the finger and face in the human somatosensory cortex

As shown in Figs. 4 and 5B, electrical stimulation of the finger or face induced optical responses along the central sulcus on the postcentral gyrus, showing a topographic representation. In the

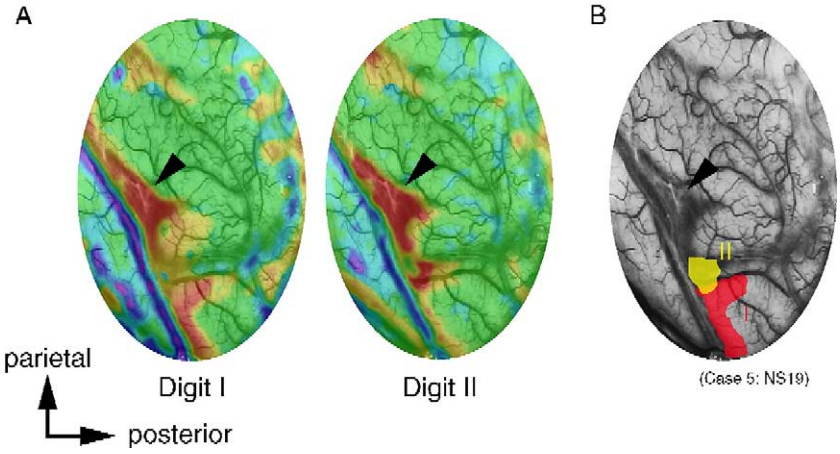

Fig. 3. An unsuccessful example of intrinsic optical imaging of Digits I–V responses. In this case, although Digits I and II stimulation induced optical signals as shown in A, large signals indicated by arrowheads seemed to be movement artifacts due to the thickened arachnoid membrane. The thickened membrane covered the region corresponding to the Digit III–V areas, so that further recordings were not made. In B, the response areas of Digits I and II are shown on the vascular image in red and yellow, respectively.

finger response area, the fingers were sequentially represented from the latero-inferior region (Digit I) to the medio-superior region (Digit V), and in the face response area, parts of the face were aligned from the superior (N. V_1) to inferior (N. V_3) region in the somatosensory cortex. The sequential order of the finger/face representation observed in the present study is consistent with previous reports in humans using magnetoencephalography (MEG) (Nakamura et al., 1998; for a review, see Kakigi et al., 2000) and in

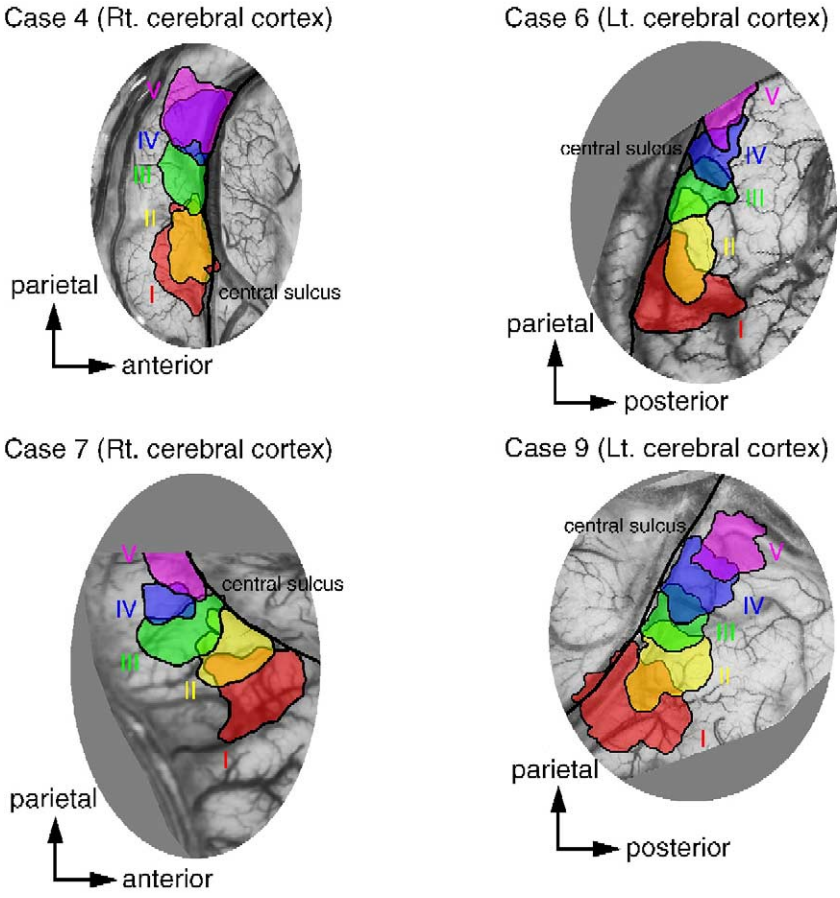

Fig. 4. Functional maps of finger representations in the somatosensory cortex obtained from four different patients (Case 4, 6, 7 and 9 in Table 1). The optical response area for each finger stimulation was defined as the area with the fractional change ($\Delta R/R$) > 1.5×10^{-3}. The response areas of different fingers are shown with different translucent colors (Digit I: red; Digit II: yellow; Digit III: green; Digit IV: blue; Digit V: red purple), and are superimposed on the vascular image. Each response area is outlined with a black solid curve. Maps were obtained from the right (Case 4 and 7) and left (Case 6 and 9) cortices.

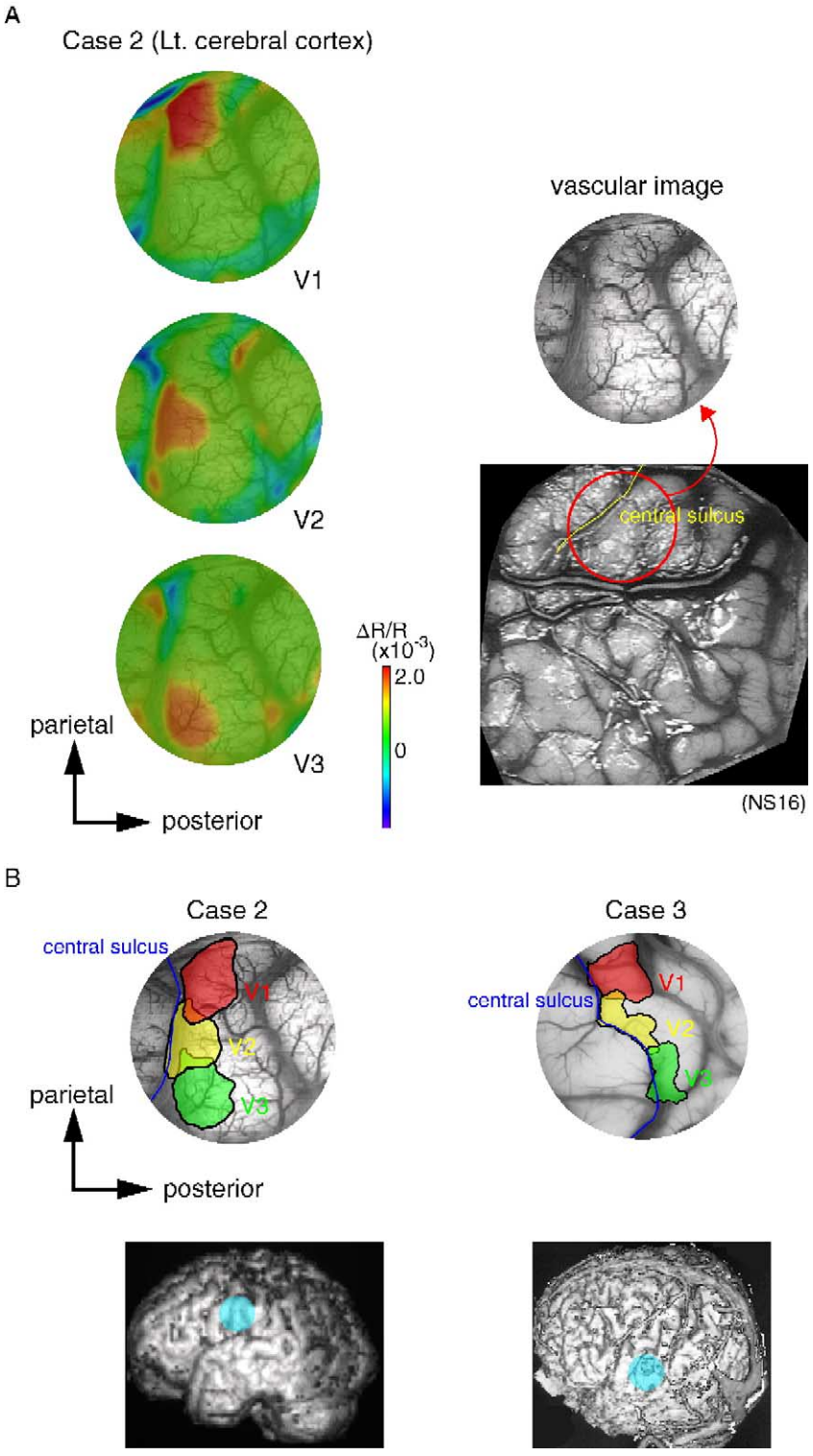

Fig. 5. Intrinsic optical images and maps of the face region in the somatosensory cortex. (A) Optical responses induced by supraorbital (N. V_1), zygomaticofacial (N. V_2) and mental (N. V_3) nerve stimulation in a 19-year-old patient (Case 2 in Table 1). The optical responses are illustrated with pseudo-color images superimposed on the vascular image. The vascular image and the recording site (indicated by a red circle) are shown in the right panels. The yellow line on the lower right photograph shows the central sulcus. (B) Functional maps of face representations in the somatosensory cortex obtained from two patients (Cases 2 and 3 in Table 1). The optical response area for each stimulation was defined as the area with the fractional change ($\Delta R/R$) > 1.5×10^{-3}. The response areas of different nerves are shown with different translucent colors (N. V_1: red; N. V_2: yellow; N. V_3: green), and are superimposed on the vascular image. Each response area is outlined with a black solid curve. The recording site is shown on three-dimensionally reconstructed MR images with blue circles.

non-human primates using electrophysiological recording (Kaas et al., 1979; Nelson et al., 1980).

Kaas et al. (1979) showed that complete somatotopic maps are present in each Brodmann's area (3a, 3b, 1 and 2; Brodmann, 1909), using micro-electrode recording. Although it is important to determine which Brodmann's areas the response area corresponds to, it is usually difficult to identify each Brodmann's area based on macroanatomical landmarks. Geyer et al. (1999, 2000) developed an observer-independent and statistically-testable procedure to identify cytoarchitectonic borders of Brodmann's subdivisions, and showed that Brodmann's area 1 in the human brain occupies the crown of the postcentral gyrus and reaches down into the postcentral sulcus. Comparing their maps together with Brodmann's original maps (Brodmann, 1909), it is reasonable to consider that the optical response area along the central sulcus correspond to Brodmann's area 1.

Concerning the finger and face representations in the somatosensory cortex, we extracted two interesting characteristics from Figs. 4 and 5B. Firstly, as shown in Cases 6, 7, and 9 of Fig. 4, Digit I showed the largest territory and Digits III–V showed smaller territories. A similar observation has been reported in Brodmann's areas 1 and 2 of the macaque monkey with the intrinsic optical imaging method (Shoham and Grinvald, 2001). These results might be due that (1) the different fingers have different number of receptors, and/or (2) the brain has given more area to the different fingers based on the amount of use by person.

Secondly, as shown in Fig. 4, the response areas of each finger overlapped each other. In electrophysiological studies using awake behaving monkeys, it was reported that individual neurons in the somatosensory cortex respond to multiple digits (Favorov and Whitsel, 1988a,b; Gardner, 1988; Iwamura et al., 1983a,b). Similar results have also been observed using the intrinsic optical imaging technique in anesthetized animals. Shoham and Grinvald (2001) observed significant overlaps between activations evoked by neighboring fingers in Brodmann's area 1 of macaque monkeys, and Chen et al. (2001) observed the overlap of optical responses in Brodmann's area 3b of squirrel monkeys. In the human cortex, Cannestra et al. (1998) reported overlapping responses between the thumb, index, and middle fingers. Krause et al. (2001) also observed representational overlaps of the index and middle fingers in multiple areas of the primary somatosensory cortex using a functional MRI (fMRI) method. As shown in Fig. 5, the face response areas in the somatosensory cortex also partially overlapped each other. However, the extent of the overlap in the face region was smaller than that in the finger region. This might be because stimulation was applied to part of the branches of the trigeminal nerve (supraorbital, zygomaticofacial, and mental branch). In the study of Schwartz et al. (2004), significant overlaps of the upper and lower face regions were reported in a single case study. Considering the results obtained in the present study together with hitherto reported observations, the overlap of the activated areas seems to be a common feature in the somatosensory cortex not only in non-human animals, but also in humans. This overlap might be functionally important in sensory information processing.

For the overlapping of the response area, there is another possibility. The optical responses obtained at a wavelength of 605 nm likely represents vascular changes, such as oximetry and blood volume (Bonhoeffer and Grinvald, 1996,b; Nemoto et al., 2004; Sheth et al., 2004a). Over the 5-s sampling period, the 'vascular overspill' may occur as a result of the spreading (or conduction) of vascular responses to feeding vessels common to neighboring cortical areas. Although electrophysiological studies suggest that neuronal responses may indeed overlap (Favorov and Whitsel, 1988a,b; Gardner, 1988; Iwamura et al., 1983a,b), the origin of the overlap of optical responses may be predominantly vascular rather than neuronal, and its functional significance requires further determination.

The difference between the monkey and human somatosensory cortices

As described in the previous session, functional representation of the somatosensory cortex was basically the same between monkeys and humans. One difference was the lack of a "common patch" in the human cortex, which was reported by Shoham and Grinvald (2001) in the macaque monkey. Applying intrinsic optical imaging to the monkey primary somatosensory cortex, they found that stimulation of the fingers evoked activity not only in the expected somatotopic position within the hand area, but also in the adjacent "common patch" region, which was located just medially to the fingers region. This area corresponds to the region representing the ulnar volar pads (Nelson et al., 1980; Pons et al., 1985), and they suggested that the common patch may be dominated by inputs from very sensitive Pacinian receptors.

In our human study, responses like the "common patch" were not observed in every case. This might indicate a difference in functional representation of the somatosensory cortex between monkeys and humans. Another possibility is that the result was due to a difference in the stimulation paradigm: we used electrical stimulation, whereas Shoham and Grinvald (2001) used tactile stimulation. Cannestra et al. (1998) used finger tip vibratory stimulation with intraoperative optical imaging, but they did not describe the "common patch" in the human somatosensory cortex, either.

Intraoperative intrinsic optical imaging and its application limitations

Among several functional brain imaging techniques, intrinsic optical imaging has the best combination of spatial and temporal resolutions for mapping the functional topography of the human cortex (Pouratian et al., 2003). Recently, many researchers have become aware of the usefulness of this technique, and its applications are expanding from the somatosensory cortex (Cannestra et al., 1996, 1998, 2001; Sato et al., 2002; Schwartz et al., 2004; Shoham and Grinvald, 2001; Toga et al., 1995) to the motor cortex (Pouratian et al., 2002) and the language centers (Cannestra et al., 2000; Haglund et al., 1992; Pouratian et al., 2000). Intrinsic optical imaging has also been used to detect the spread of epileptic waves (Haglund and Hochman, 2004; Haglund et al., 1992). In the present study, we applied this optical technique to nine patients, and succeeded in recording optical responses from every case except for one patient (Case 1 in Table 1), who suffered from hemiplegia with loss of the SEP responses. These results imply that intraoperative intrinsic optical imaging is a powerful technique to evaluate human brain functions.

Here, we noted one limitation in applying this optical imaging technique to human patients. As shown in Fig. 3A, a case in which the arachnoid membrane was thickened, it was a difficult task to rule out movement artifacts from the true signals. The arachnoid membrane is often thickened in brain tumor patients, especially in

elderly persons, and it is necessary to carefully consider the condition of the brain before optical imaging. In the present study, we tried to reduce movements of the thickened membrane with a glass plate, but it was not successful. It might be useful to use longer wavelengths for illumination or post-acquisition image registration (Cannestra et al., 1998; Pouratian et al., 2003) to overcome this problem.

Acknowledgments

We are grateful to Dr. Amiram Grinvald for generous help in constructing the optical recording apparatus, and to reviewers for their helpful comments about our manuscript. We also wish to express our gratitude to Drs. Kohtaro Kamino and Kimiyoshi Hirakawa for helpful discussions throughout the course of our work, and many medical doctors and nurses for their kind cooperation in the operating room. This research was supported by grants from the Monbu-Kagaku-Sho of Japan and research funds from the Shimadzu Science Foundation, Nissan Science Foundation, Takeda Science Foundation and Japan Epilepsy Research Foundation.

References

Bonhoeffer, T., Grinvald, A., 1993. The layout of iso-orientation domains in area 18 of cat visual cortex: optical imaging reveals a pinwheel-like organization. J. Neurosci. 13, 4157–4180.

Bonhoeffer, T., Grinvald, A., 1996. Optical imaging based on intrinsic signals: the methodology. In: Toga, A.W., Mazziotta, J.C. (Eds.), Brain Mapping: the Methods. Academic Press, California, pp. 55–97.

Brodmann, K., 1909. Vergleichende Lokalisationslehre der Großhirnrinde. Barth JA, Leipzig.

Cannestra, A.F., Blood, A.J., Black, K.L., Toga, A.W., 1996. The evolution of optical signals in human and rodent cortex. NeuroImage 3, 202–208.

Cannestra, A.F., Black, K.L., Martin, N.A., Cloughesy, T., Burton, J.S., Rubinstein, E., Woods, R.P., Toga, A.W., 1998. Topological and temporal specificity of human intraoperative optical intrinsic signals. NeuroReport 9, 2557–2563.

Cannestra, A.F., Bookheimer, S.Y., Pouratian, N., O'Farrell, A., Sicotte, N., Martin, N.A., Becker, D., Rubino, G., Toga, A.W., 2000. Temporal and topological characterization of language cortices using intraoperative optical intrinsic signals. NeuroImage 12, 41–54.

Cannestra, A.F., Pouratian, N., Bookheimer, S.Y., Martin, N.A., Becker, D.P., Toga, A.W., 2001. Temporal spatial differences observed by functional MRI and human intraoperative optical imaging. Cerebr. Cortex 11, 773–782.

Chapman, B., Stryker, M.P., Bonhoeffer, T., 1996. Development of orientation preference maps in ferret primary visual cortex. J. Neurosci. 15, 6443–6453.

Chen, L.M., Friedman, R.M., Ramsden, B.M., LaMotte, R.H., Roe, A.W., 2001. Fine-scale organization of S1 (Area 3b) in the squirrel monkey revealed with intrinsic optical imaging. J. Neurophysiol. 86, 3011–3029.

Cohen, L.B., 1973. Changes in neuron structure during action potential propagation and synaptic transmission. Physiol. Rev. 53, 373–418.

Dowling, J.L., Henegar, M.M., Liu, D., Rovainen, C.M., Woolsey, T.A., 1996. Rapid optical imaging of whisker responses in the rat barrel cortex. J. Neurosci. Methods 66, 113–122.

Favorov, O., Whitsel, B.L., 1988a. Spatial organization of the peripheral input to area 1 cell columns: I. The detection of "segregates". Brain Res. Rev. 13, 25–42.

Favorov, O., Whitsel, B.L., 1988b. Spatial organization of the peripheral input to area 1 cell columns: II. The forelimb representation achieved by a mosaic of segregates. Brain Res. Rev. 13, 43–56.

Frostig, R.D., Lieke, E.E., Ts'o, D.Y., Grinvald, A., 1990. Cortical functional architecture and local coupling between neuronal activity and the microcirculation revealed by in vivo high-resolution optical imaging of intrinsic signals. Proc. Natl. Acad. Sci. U. S. A. 87, 6082–6086.

Gardner, E.P., 1988. Somatosensory cortical mechanisms of feature detection in tactile and kinesthetic discrimination. Can. J. Physiol. Pharm. 66, 439–454.

Geyer, S., Schleicher, A., Zilles, K., 1999. Areas 3a, 3b, and 1 of human primary somatosensory cortex 1. Microstructural organization and interindividual variability. NeuroImage 10, 63–83.

Geyer, S., Schormann, T., Mohlberg, H., Zilles, K., 2000. Areas 3a, 3b, and 1 of human primary somatosensory cortex 2. Spatial normalization to standard anatomical space. NeuroImage 11, 684–696.

Gochin, P.M., Bedenbaugh, P., Gelfand, J.J., Gross, C.G., Gerstein, G.L., 1992. Intrinsic signal optical imaging in the forepaw area of rat somatosensory cortex. Proc. Natl. Acad. Sci. U. S. A. 89, 8381–8383.

Gödecke, I., Bonhoeffer, T., 1996. Development of identical orientation maps for two eyes without common visual experience. Nature 379, 251–254.

Grinvald, A., Lieke, E., Frostig, R.D., Gilbert, C.D., Wiesel, T.N., 1986. Functional architecture of cortex revealed by optical imaging of intrinsic signals. Nature 324, 361–364.

Haglund, M.M., Hochman, D.W., 2004. Optical imaging of epileptiform activity in human neocortex. Epilepsia 45 (Suppl. 4), 43–47.

Haglund, M.M., Ojemann, G.A., Hochman, D.W., 1992. Optical imaging of epileptiform and functional activity in human cerebral cortex. Nature 358, 668–671.

Iwamura, Y., Tanaka, M., Sakamoto, M., Hikosaka, O., 1983a. Functional subdivision representing different finger regions in area 3 of the first somatosensory cortex of the conscious monkey. Exp. Brain Res. 51, 315–326.

Iwamura, Y., Tanaka, M., Sakamoto, M., Hikosaka, O., 1983b. Converging patterns of finger representation and complex response properties of neurons in area 1 of the first somatosensory cortex of the conscious monkey. Exp. Brain Res. 51, 327–337.

Kaas, J.H., Nelson, R.J., Sur, M., Lin, C.S., Merzenich, M.M., 1979. Multiple representations of the body within the primary somatosensory cortex of primates. Science 204, 521–523.

Kakigi, R., Hoshiyama, M., Shimojo, M., Naka, D., Yamasaki, H., Watanabe, S., Xiang, J., Maeda, K., Lam, K., Itomi, K., Nakamura, A., 2000. The somatosensory evoked magnetic fields. Prog. Neurobiol. 61, 495–523.

Krause, T., Kurth, R., Ruben, J., Schwiemann, J., Villringer, K., Deuchert, M., Moosmann, M., Brandt, S., Wolf, K.-J., Curio, G., Villringer, A., 2001. Representational overlap of adjacent fingers in multiple areas of human primary somatosensory cortex depends on electrical stimulus intensity: an MRI study. Brain Res. 899, 36–46.

Malonek, D., Grinvald, A., 1996. Interactions between electrical activity and cortical microcirculation revealed by imaging spectroscopy: implications for functional brain mapping. Science 272, 551–554.

Masino, S.A., Kwon, M.C., Dory, Y., Frostig, R.D., 1993. Characterization of functional organization within rat barrel cortex using intrinsic signal optical imaging through a thinned skull. Proc. Natl. Acad. Sci. U. S. A. 90, 9998–10002.

Nakamura, A., Yamada, T., Goto, A., Kato, T., Ito, K., Abe, Y., Kachi, T., Kakigi, R., 1998. Somatosensory homunculus as drawn by MEG. NeuroImage 7, 377–386.

Nelson, R.J., Sur, M., Felleman, D.J., Kaas, J.H., 1980. Representations of the body surface in postcentral parietal cortex of *Macaca fascicularis*. J. Comp. Neurol. 192, 611–643.

Nemoto, M., Sheth, S., Guiou, M., Pouratian, N., Chen, J.W.Y., Toga, A.W., 2004. Functional signal- and paradigm-dependent linear relationships between synaptic activity and hemodynamic responses in rat somatosensory cortex. J. Neurosci. 24, 3850–3861.

Nuwer, M.R., Banoczi, W.R., Cloughesy, T.F., Hoch, D.B., Peacock, W., Levesque, M.F., Black, K.L., Martin, N.A., Becker, D.P., 1992.

Topographic mapping of somatosensory evoked potentials helps identify motor cortex more quickly in the operating room. Brain Topogr. 5, 53–58.

Penfield, W., Boldray, E., 1937. Somatic motor and sensory representation in the cerebral cortex of man as studied by electrical stimulation. Brain 60, 389–443.

Pons, T.P., Garraghty, P.E., Cusick, C.G., Kaas, J.H., 1985. The somatotopic organization of area 2 in macaque monkeys. J. Comp. Neurol. 241, 445–466.

Pouratian, N., Bookheimer, S.Y., O'Farrell, A.M., Sicotte, N.L., Cannestra, A.F., Becker, D., Toga, A.W., 2000. Optical imaging of bilingual cortical representations. J. Neurosurg. 93, 676–681.

Pouratian, N., Sicotte, N.L., Rex, D., Martin, N.A., Becker, D., Cannestra, A.F., Toga, A.W., 2002. Spatial/temporal correlation of BOLD and optical intrinsic signals in humans. Magn. Reson. Med. 47, 766–776.

Pouratian, N., Sheth, S.A., Martin, N.A., Toga, A.W., 2003. Shedding light on brain mapping: advances in human optical imaging. Trends Neurosci. 26, 277–282.

Sasaki, S., Yazawa, I., Miyakawa, N., Mochida, H., Shinomiya, K., Kamino, K., Momose-Sato, Y., Sato, K., 2002. Optical imaging of intrinsic signals induced by peripheral nerve stimulation in the in vivo rat spinal cord. NeuroImage 17, 1240–1255.

Sasaki, S., Sato, K., Shinomiya, K., Momose-Sato, Y., 2003. Postnatal changes in intrinsic optical responses to peripheral nerve stimulation in the in vivo rat spinal cord. NeuroImage 20, 2126–2134.

Sato, K., Nariai, T., Sasaki, S., Yazawa, I., Mochida, H., Miyakawa, N., Momose-Sato, Y., Kamino, K., Ohta, Y., Hirakawa, K., Ohno, K., 2002. Intraoperative intrinsic optical imaging of neuronal activity from subdivisions of the human primary somatosensory cortex. Cereb. Cortex 12, 269–280.

Schwartz, T.H., Chen, L.M., Freidman, R.M., Spencer, D.D., Roe, A.W., 2004. Intraoperative optical imaging of human face cortical topography: a case study. NeuroReport 15, 1527–1531.

Sheth, S.A., Nemoto, M., Guiou, M., Walker, M., Pouratian, N., Hageman, N., Toga, A.W., 2004a. Linear and nonlinear relationships between neuronal activity, oxygen metabolism, and hemodynamic responses. Neuron 42, 347–355.

Sheth, S.A., Nemoto, M., Guiou, M., Walker, M., Pouratian, N., Hageman, N., Toga, A.W., 2004b. Columnar specificity of microvascular oxygenation and volume responses: implications for functional brain mapping. J. Neurosci. 24, 634–641.

Shoham, D., Grinvald, A., 2001. The cortical representations of the hand in macaque and human area S-I: high resolution optical imaging. J. Neurosci. 21, 6820–6835.

Tanaka, T., Yazawa, I., Sato, K., Momose-Sato, Y., Kamino, K., 2000. Consistency behind trial-to-trial variations in intrinsic optical responses to single-whisker movement in the rat D1-barrel cortex. Neurosci. Res. 36, 193–207.

Toga, A.W., Cannestra, A.F., Black, K.L., 1995. The temporal/spatial evolution of optical signals in human cortex. Cereb. Cortex 5, 561–565.

Ts'o, D.Y., Frostig, R.D., Lieke, E.E., Grinvald, A., 1990. Functional organization of primate visual cortex revealed by high resolution optical imaging. Science 249, 417–420.

Yazawa, I., Sato, K., Tanaka, T., Momose-Sato, Y., Kamino, K., 1999. Intrinsic optical imaging of neural responses in in vivo rat brainstem evoked by vagus nerve stimulation. Neurosci. Res. 23, S106.

Yazawa, I., Sasaki, S., Mochida, H., Kamino, K., Momose-Sato, Y., Sato, K., 2001. Developmental changes in trial-to-trial variations in whisker barrel responses studied using intrinsic optical imaging: comparison between normal and de-whiskered rats. J. Neurophysiol. 86, 392–401.